Alkylidyne (carbaborane) complexes of the Group 6 metals. 9. The closo to hyper-closo transformations in a tungstacarborane cage system: crystal structure of [NEt4][W2(.mu.-CC6H4Me-4)(CO)2(.eta.5-7,8-Me2-7,8-C2B9H9)[.eta.6-7,8-Me2-7,8-C2B9H8-10-(CH2C6H4Me-4)]]

Nicholas Carr, Donald F. Mullica, Eric L. Sappenfield, and F. Gordon A. Stone

Organometallics, **1992**, 11 (11), 3697-3704• DOI: 10.1021/om00059a037 • Publication Date (Web): 01 May 2002

Organometallics is published by the American Chemical Society. 1155 Sixteenth Street N.W., Washington, DC 20036

Organometallics 1992, *11*, 3697-3704

Closo to Hyper-closo Transformations in a Tungstacarborane Cage System: Crystal Structure of $[NEt_4][W_2(\mu\text{-}CC_6H_4Me\text{-}4)(CO)_2(\eta^5\text{-}7,8\text{-}Me_2\text{-}7,8\text{-}C_2B_9H_9)\{\eta^6\text{-}7,8\text{-}Me_2\text{-}7,8\text{-}C_2B_9H_8\text{-}10\text{-}(CH_2C_6H_4Me\text{-}4)\}]$[†,1]

Nicholas Carr, Donald F. Mullica, Eric L. Sappenfield, and F. Gordon A. Stone*

Department of Chemistry, Baylor University, Waco, Texas 76798-7348

Received June 12, 1992

Protonation ($HBF_4{\cdot}Et_2O$) of the salts $[NEt_4][W(\equiv CR)(CO)_2(\eta^5\text{-}7,8\text{-}Me_2\text{-}7,8\text{-}C_2B_9H_9)]$ (R = Me or C_6H_4Me-4) with 0.5 mol equiv of acid affords the species $[NEt_4][W_2(\mu\text{-}CR)(CO)_2(\eta^5\text{-}7,8\text{-}Me_2\text{-}7,8\text{-}C_2B_9H_9)\{\eta^6\text{-}7,8\text{-}Me_2\text{-}7,8\text{-}C_2B_9H_8\text{-}10\text{-}(CH_2R)\}]$ (**10**). The structure of the salt **10a** (R = C_6H_4Me-4) has been established by X-ray crystallography. Crystals are monoclinic, space group $P2_1/n$ (No. 14) with a = 15.4967 (8) Å, b = 21.2541 (7) Å, c = 15.7528 (9) Å, β = 118.276 (5)°, and Z = 4. In the anion of the salt the metal–metal bond [2.683 (1) Å] is asymmetrically bridged by the p-tolylmethylidyne group [μ-C–W 1.999 (7) and 2.119 (7) Å]. One tungsten atom carries two CO groups and is part of a *closo*-C_2B_9W cage. The BH group which is in the β site with respect to the carbon atoms of the CCBBB ring adjacent to this tungsten vertex forms an exopolyhedral $B\text{–}H{\rightarrow}W$ bond to the other tungsten atom. A novel feature of the structure relates to the geometry of the other C_2B_9W cage which is no longer a closo icosahedron. Thus, the CMe groups of the cage have separated so that the C⋯C distance (2.917 Å) is no longer bonding and six atoms (CBBBCB), rather than the five found in the parent alkylidyne(carborane) complex, ligate the tungsten vertex. Thus, the distortion from icosahedral geometry leads to a hyper-closo geometry. The species **10** are formed via the thermally unstable salts $[NEt_4][W_2\{\mu\text{-}\eta^2\text{-}C(R)CO\}(CO)_2(\eta^5\text{-}7,8\text{-}Me_2\text{-}7,8\text{-}C_2B_9H_9)\{\eta^6\text{-}7,8\text{-}Me_2\text{-}7,8\text{-}C_2B_9H_8\text{-}10\text{-}(CH_2R)\}]$ (**12**), containing a bridging η^2-ketenyl group, by loss of CO. The *hyper-closo*-C_2B_9W cages in the μ-alkylidyne species **10** are transformed to a closo geometry upon treatment with $CNBu^t$ to give the compounds $[NEt_4][W_2(\mu\text{-}CR)(CNBu^t)(CO)_2(\eta^5\text{-}7,8\text{-}Me_2\text{-}7,8\text{-}C_2B_9H_9)\{\eta^5\text{-}7,8\text{-}Me_2\text{-}7,8\text{-}C_2B_9H_8\text{-}10\text{-}(CH_2R)\}]$ (**13**). Protonation of **13a** (R = C_6H_4Me-4) leads to coupling of the initially formed aminocarbyne group with the μ-p-tolylmethylidyne ligand to give the species $[W_2\{\mu\text{-}C(C_6H_4Me\text{-}4)CN(H)Bu^t\}(CO)_2(\eta^5\text{-}7,8\text{-}Me_2\text{-}7,8\text{-}C_2B_9H_9)\{\eta^5\text{-}7,8\text{-}Me_2\text{-}7,8\text{-}C_2B_9H_8\text{-}10\text{-}(CH_2C_6H_4Me\text{-}4)\}]$ (**14**) in which the two metal centers are asymmetrically spanned by an aminoalkyne ligand. In addition to the X-ray diffraction study the synthesis and spectroscopic properties of the new metallacarborane cluster compounds are reported and discussed.

Introduction

In a series of recent articles[1,2] we have described protonation studies of salts of the anionic alkylidyne(carborane) tungsten complexes $[W(\equiv CR)(CO)_2(\eta^5\text{-}7,8\text{-}R'_2\text{-}7,8\text{-}C_2B_9H_9)]^-$ (**1**) (R = alkyl, aryl, alkynyl; R′ = H or Me), $[W(\equiv CC\equiv CBu^t)(CO)_2(\eta^5\text{-}7,9\text{-}C_2B_9H_{11})]^-$ (**2**), and $[W(\equiv CC_6H_4Me\text{-}4)(CO)_2(\eta^6\text{-}7,9\text{-}Me_2\text{-}7,9\text{-}C_2B_{10}H_{10})]^-$ (**3**). We have previously noted that the choice of acid (HBF_4 vs HI), alkylidyne group, and carborane cage ($7,8\text{-}C_2B_9H_{11}$ vs $7,8\text{-}Me_2\text{-}7,8\text{-}C_2B_9H_9$ vs $7,9\text{-}Me_2\text{-}7,9\text{-}C_2B_{10}H_{10}$) is important in directing the course of these reactions from which many different types of compounds have consequently been obtained.

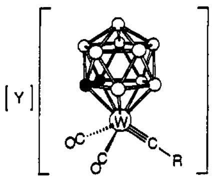

	R	●
1a	C_6H_4Me-4	CMe
1b	Me	CMe
1c	$C\equiv CBu^t$	CMe
1d	C_6H_4OMe-2	CMe
1e	$C_6H_4CH_2OMe$-2	CMe
1f	C_6H_4Me-4	CH
1g	$C\equiv CBu^t$	CH

Y = NEt_4, PPh_4, $AsPh_4$, NMe_3Ph, $N(PPh_3)_2$, *etc.*

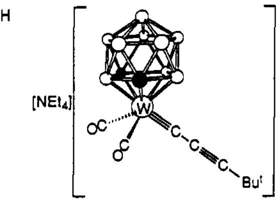

2

● CH

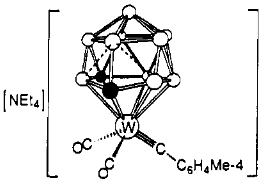

3

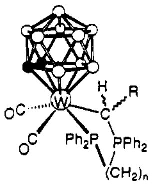

	R	n
4a	C_6H_4Me-4	1
4b	C_6H_4Me-4	2
4c	C_6H_4OMe-2	1

It is becoming increasingly evident that the first step in these protonation reactions is formation of a highly reactive alkylidene species $[M\{=C(H)R\}(CO)_2(\eta^x\text{-}C_2B_nH_nR'_2)]$ (x = 5, n = 9; x = 6, n = 10). Indeed, under certain conditions it has proven possible to trap these intermediates in the form of ylide complexes of the type $[W(CO)_2\{CH(R)PPh_2(CH_2)_mPPh_2\}(\eta^5\text{-}7,8\text{-}Me_2\text{-}7,8\text{-}C_2B_9H_9)]$ (**4**, R = C_6H_4Me-4, Me, C_6H_4OMe-2; m = 1,2).[2d,3] However, for the reagents **1** containing the methyl-substituted cage, $7,8\text{-}Me_2\text{-}7,8\text{-}C_2B_9H_9$, a more common outcome of such reactions is migration and insertion of the alkylidene group into a B—H bond of the carborane cage. Thus, protona-

---

* To whom correspondence should be addressed.

[†] In the compounds described in this paper a tungsten atom and a $[nido\text{-}7,8\text{-}C_2B_9H_9\text{-}7,8\text{-}Me_2]^{2-}$ anion form a *closo-* or *hyper-closo*-1,2-dicarba-3-tungstadodecacarborane structure. However, use of this numbering scheme leads to an impossibly complex nomenclature for the dimetal compounds reported. We therefore treat the cages as nido 11-vertex ligands with numbering as for an icosahedron from which the twelfth vertex has been removed.

(1) This article may be considered as part 9 in the series Alkylidyne(carbaborane) Complexes of the Group 6 Metals. For Part 8 see ref 2a.

0276-7333/92/2311-3697$03.00/0

Table I. Physical and Infrared Absorption Data[a]

	compd	color	yield/%	$\nu_{max}(CO)^b$/cm^{-1}
10a	[NEt$_4$][W$_2$(μ-CC$_6$H$_4$Me-4)(CO)$_2$(η^5-7,8-Me$_2$-7,8-C$_2$B$_9$H$_9$){η^6-7,8-Me$_2$-7,8-C$_2$B$_9$H$_8$-10-(CH$_2$C$_6$H$_4$Me-4)}]	orange	31	1982 (vs), 1917 (s)
10b	[NEt$_4$][W$_2$(μ-CMe)(CO)$_2$(η^5-7,8-Me$_2$-C$_2$B$_9$H$_9$)(η^6-7,8-Me$_2$-7,8-C$_2$B$_9$H$_8$-10-Et)]	orange	32	1973 (vs), 1903 (s)
12a	[NEt$_4$][W$_2${μ-η^2-C(C$_6$H$_4$Me-4)CO}(CO)$_2$(η^5-7,8-Me$_2$-7,8-C$_2$B$_9$H$_9$){η^6-7,8-Me$_2$-7,8-C$_2$B$_9$H$_8$-10-(CH$_2$C$_6$H$_4$Me-4)}]	red	*c*	1980 (vs), 1906 (s), 1753 (w, br)
13a	[NEt$_4$][W$_2$(μ-CC$_6$H$_4$Me-4)(CNBu^t)(CO)$_2$(η^5-7,8-Me$_2$-7,8-C$_2$B$_9$H$_9$){η^5-7,8-Me$_2$-7,8-C$_2$B$_9$H$_8$-10-(CH$_2$C$_6$H$_4$Me-4)}]	brown	90	1944 (vs), 1874 (s), 2110 (w, br)^d
13b	[NEt$_4$][W$_2$(μ-CMe)(CNBu^t)(CO)$_2$(η^5-7,8-Me$_2$-7,8-C$_2$B$_9$H$_9$){η^5-7,8-Me$_2$-7,8-C$_2$B$_9$H$_8$-10-Et)}]	brown	80	1938 (vs), 1869 (s), 2109 (w, br)^d
14	[W$_2${μ-C(C$_6$H$_4$Me-4)CN(H)Bu^t}(CO)$_2$(η^5-7,8-Me$_2$-7,8-C$_2$B$_9$H$_9$){η^5-7,8-Me$_2$-7,8-C$_2$B$_9$H$_8$-10-(CH$_2$C$_6$H$_4$Me-4)}]	blue	56	2027 (s), 1978 (s), 1596 (w, br)^d

[a] Satisfactory analytical data (C, H, N) have been obtained (see Experimental Section) for all new compounds except **12a**. [b] All complexes show a weak, very broad absorption at ~2550 cm^{-1} due to BH stretching. Legend: vs, very strong; s, strong; w, weak; br, broad. [c] Decomposed to give complex **13a**, hence not isolated in pure form (see text). [d] ν_{max}(CN).

tion of the salts **1a–1e** in the presence of donor molecules L (CO, PPh$_3$, or PhC$_2$Ph), affords compounds of the general type [W(CO)$_2$(L)$_2${η^5-7,8-Me$_2$-7,8-C$_2$B$_9$H$_8$-10-(CH$_2$R)}] (**5**)[4] or [W(CO)$_2$(L)$_2${η^5-7,8-Me$_2$-7,8-C$_2$B$_9$H$_7$-5,10-(CH$_2$C$_6$H$_4$CH$_2$-2)}] (**6**),[2b] the latter species resulting from elimination of MeOH through activation of a second B—H bond.

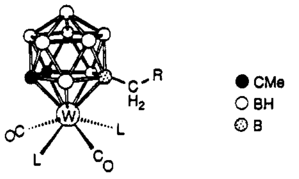

	R	L
5a	C$_6$H$_4$Me-4	CO
5b	Me	CO
5c	C$_6$H$_4$OMe-2	CO
5d	C$_6$H$_4$Me-4	PPh$_3$
5e	C$_6$H$_4$Me-4	PhC$_2$Ph

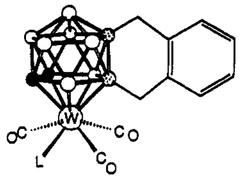

	L
6a	CO
6b	PHPh$_2$

In contrast, the B—H bonds in complexes having the unsubstituted C$_2$B$_9$H$_{11}$ cage system appear much less active toward insertion of the alkylidene group, though at present there are relatively few examples where a direct comparison can be made. This leads to reaction types in which the initially formed alkylidene ligand couples with other unsaturated groups or is released altogether. For example, protonation of an equimolar mixture of **1g** and [M(≡CC$_6$H$_4$Me-4)(CO)$_2$(η-C$_5$H$_5$)] (M = Mo or W) affords the dimetal complexes [MW{μ-η^3-C(Bu^t)CC[=C(H)C$_6$H$_4$Me-4]}(CO)$_4$(η-C$_5$H$_5$)(η^5-7,8-C$_2$B$_9$H$_{11}$)] (**7**),[2a] whilst protonation of **1f** in the presence of [W(≡CMe)(CO)$_2$(η-C$_5$H$_5$)] gives [W$_2$(μ-CC$_6$H$_4$Me-4)(CO)$_3$(η-C$_5$H$_5$)(η^5-7,8-C$_2$B$_9$H$_{11}$)] (**8**).[2c] The former reaction involves coupling of the alkylidyne group of the cyclopentadienyl species with an initially formed alkylidene W=C(H)R group on the carborane species, whilst the latter involves formal loss of a C(H)Me moiety. Furthermore, we have previously shown[5] that protonation of **1f** [Y = N(PPh$_3$)$_2$] with HBF$_4$·Et$_2$O gives the salt [N(PPh$_3$)$_2$][W$_2$(μ-H){μ-C$_2$(C$_6$H$_4$Me-4)$_2$}(CO)$_4$(η^5-7,8-C$_2$B$_9$H$_{11}$)$_2$] (**9**), containing a bridging alkyne ligand, irrespective of the amount of acid employed. This contrasts with the nature of the products [W(CO)$_4${η^5-7,8-Me$_2$-7,8-C$_2$B$_9$H$_8$-10-(CH$_2$R)}] (R = C$_6$H$_4$Me-4 (**5a**); R = Me (**5b**)), obtained upon treatment of the 7,8-Me$_2$ substituted cage analog **1a** with 1 molar equiv of HBF$_4$·Et$_2$O.[4]

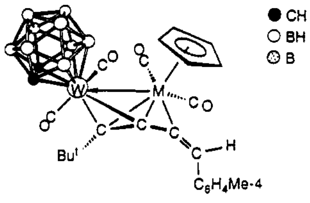

	M
7a	W
7b	Mo

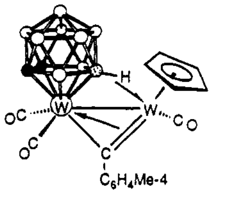

8

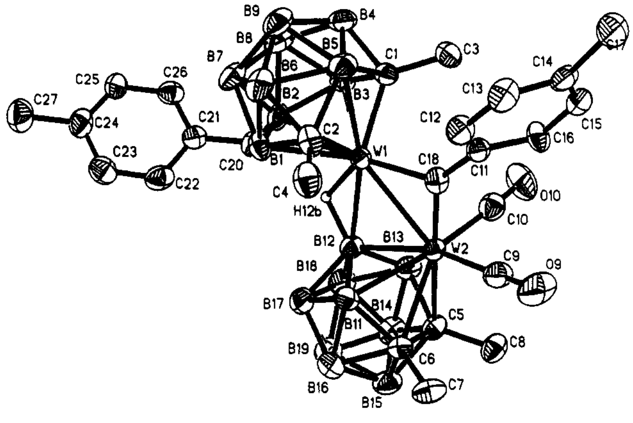

Figure 1. Structure of the anion of [NEt$_4$][W$_2$(μ-CC$_6$H$_4$Me-4)(CO)$_2$(η^5-7,8-Me$_2$-7,8-C$_2$B$_9$H$_9$){η^6-7,8-Me$_2$-7,8-C$_2$B$_9$H$_8$-10-(CH$_2$C$_6$H$_4$Me-4)}] (**10a**) (40% thermal ellipsoids), showing the crystallographic labeling scheme.

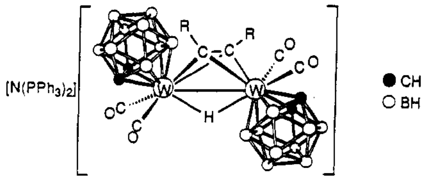

9 R = C$_6$H$_4$Me-4

In this paper we describe the synthesis of some novel dimetal species obtained from the salts [NEt$_4$][W(≡CR)(CO)$_2$(η^5-7,8-Me$_2$-7,8-C$_2$B$_9$H$_9$)] (R = C$_6$H$_4$Me-4 (**1a**); R = Me (**1b**)) by employing a deficiency of the acid HBF$_4$·Et$_2$O.

Results and Discussion

The reaction between **1a** (Y = NEt$_4$) and ca. 0.5 mol equiv of HBF$_4$·Et$_2$O in CH$_2$Cl$_2$ affords the orange salt

---

(2) (a) Bruce, G. A.; Mullica, D. F.; Sappenfield, E. L.; Stone, F. G. A. *J. Chem. Soc., Dalton Trans.*, in press. (b) Jeffery, J. C.; Li, S.; Stone, F. G. A. *Organometallics* **1992**, *11*, 1902. (c) Brew, S. A.; Jeffery, J. C.; Mortimer, M. C.; Stone, F. G. A. *J. Chem. Soc., Dalton Trans.* **1992**, 1365. (d) Jeffery, J. C.; Li, S.; Sams, D. W. I.; Stone, F. G. A. *J. Chem. Soc., Dalton Trans.* **1992**, 877 and references cited herein.

(3) Brew, S. A.; Jenkins, P. D.; Jeffery, J. C.; Stone, F. G. A. *J. Chem. Soc., Dalton Trans.* **1992**, 401.

(4) Brew, S. A.; Devore, D. D.; Jenkins, P. D.; Pilotti, M. U.; Stone, F. G. A. *J. Chem. Soc., Dalton Trans.* **1992**, 393.

(5) James, A. P.; Stone, F. G. A. *J. Organomet. Chem.* **1986**, *310*, 47.

Table II. Hydrogen-1 and Carbon-13 NMR Data[a]

compd	^{1}H/δ (J/Hz)	^{13}C/δ[b]
10a[c,d]	1.09 (br, 12 H, $NCH_2\mathit{Me}$), 1.93 (s, 6 H, CMe), 2.20 (s, 3 H, Me-4), 2.26 (s, 6 H, CMe), 2.39 (s, 3 H, Me-4), 2.82 (br, 2 H, BCH_2), 2.87 (br, 8 H, $N\mathit{CH_2}Me$), 6.74, 6.91 [$(AB)_2$, 4 H, C_6H_4, J(AB) 7], 7.24, 7.34 [$(AB)_2$, 4 H, C_6H_4, J(AB) 7]	346.7 (μ-$\mathit{C}C_6H_4Me$-4), 221.1 (s, WCO × 2), 182.7 (br, *C*Me), 158.6, 144.5 [$C^1(C_6H_4)$], 135.5, 131.8 [$C^4(C_6H_4)$], 129.7, 128.1, 127.8, 126.8 [$C^{2,3}(C_6H_4)$], 64.1 (br, *C*Me), 51.5 ($N\mathit{CH_2}Me$), 40.2 (br, BCH_2), 38.0 (C*Me*), 31.1 (C*Me*), 21.2, (Me-4), 21.1 (Me-4), 7.0 ($NCH_2\mathit{Me}$)
10b[c,d]	0.68 [t, 3 H, $BCH_2\mathit{Me}$, J(HH) 8], 1.22 (br, 12 H, $NCH_2\mathit{Me}$), 1.40 [q, 2 H, $B\mathit{CH_2}Me$, J(HH) 8], 1.95 (s, 6 H, CMe), 2.18 (s, 6 H, CMe), 3.10 (br, 8 H, $N\mathit{CH_2}Me$), 4.31 (s, 3 H, μ-CMe)	343.6 (μ-*C*Me), 216.8 (s, WCO × 2), 179.7 (br, *C*Me), 63.6 (br, *C*Me), 51.4 ($N\mathit{CH_2}Me$), 41.6 (μ-C*Me*), 34.9 (C*Me*), 31.1 (C*Me*), 23.6 (br, $B\mathit{CH_2}Me$), 14.8 ($BCH_2\mathit{Me}$), 7.1 ($NCH_2\mathit{Me}$)
12a[c,e]	1.25 [t of t, 12 H, $NCH_2\mathit{Me}$, J(HH) 7, J(NH) 2], 1.61 (s, 3 H, CMe), 1.96 (s, 3 H, Me), 2.08 (s, 3 H, Me), 2.18, (s, 3 H, Me), 2.27 (s, 3 H, Me), 2.60 (s, 3 H, Me), 2.34, 2.81 [(AB), 2 H, BCH_2, J(AB) 13], 3.11 [q, 8 H, $N\mathit{CH_2}Me$, J(HH) 7], 6.37, 6.80 [$(AB)_2$, 4 H, C_6H_4, J(AB) 8], 7.06 (m, 4 H, C_6H_4)	215.9, 213.6 (s × 2, WCO), 187.5 [μ-$C(C_6H_4)\mathit{C}O$], 184.4 (br, *C*Me), 176.5 (br, *C*Me), 145.1, 142.3 [$C^1(C_6H_4)$], 135.7, 131.7 [$C^4(C_6H_4)$], 129.0, 128.0, 127.5 [$C^{2,3}(C_6H_4)$], 94.8 [μ-$\mathit{C}(C_6H_4)CO$], 69.2 (br, *C*Me), 67.8 (br, *C*Me), 52.3 ($N\mathit{CH_2}Me$), 39.3 (C*Me*), 35.9 (br, BCH_2), 32.7 (C*Me*), 31.2 (C*Me*), 29.9 (C*Me*), 21.0 (Me-4), 20.8 (Me-4), 7.4 ($NCH_2\mathit{Me}$)
13a	−5.33 (br, 1 H, B–H→W), 1.22 (br, 21 H, $NCH_2\mathit{Me}$ and $CNCMe_3$), 1.24 (s, 3 H, CMe), 1.59 (br, 2 H, BCH_2), 1.69 (s, 3 H, CMe), 2.14 (s, 3 H, Me), 2.17 (s, 3 H, Me), 2.18 (s, 3 H, Me), 2.53 (s, 3 H, CMe), 3.03 [q, 8 H, $N\mathit{CH_2}Me$, J(HH) 7], 6.45, 6.76 [$(AB)_2$, 4 H, C_6H_4, J(AB) 8], 7.29, 7.34 [$(AB)_2$, 4 H, C_6H_4, J(AB) 8]	354.5 (μ-$\mathit{C}C_6H_4Me$-4), 223.6, 220.0 (s × 2, WCO), 166.3 [$C^1(C_6H_4)$], 161.6 ($\mathit{C}NCMe_3$), 144.9 [$C^1(C_6H_4)$], 133.8, 131.9 [$C^4(C_6H_4)$], 128.8, 128.0, 127.4, 123.4 [$C^{2,3}(C_6H_4)$], 62.5 (br, *C*Me), 61.8 (br, *C*Me), 57.6 ($CN\mathit{C}Me_3$), 53.0 (br, $N\mathit{CH_2}Me$), 34.5 (C*Me*), 32.6 (C*Me*), 32.2 (C*Me*), 31.0 ($CNC\mathit{Me_3}$), 29.9 (br, BCH_2), 29.7 (C*Me*), 21.3 (Me-4), 21.0 (Me-4), 7.8 ($NCH_2\mathit{Me}$)
13b	−5.56 [q, 1 H, B–H→W, J(BH) 73], −0.59 (m, 2 H, BCH_2), 0.26 [t, 3 H, $BCH_2\mathit{Me}$, J(HH) 8], 1.17 (s, 9 H, $CNC\mathit{Me_3}$), 1.30 [t of t, 12 H, $NCH_2\mathit{Me}$, J(HH) 7, J(NH) 2], 1.60 (s, 3 H, CMe), 1.94 (s, 3 H, CMe), 2.15 (s, 3 H, CMe), 2.19 (s, 3 H, CMe), 3.16 [q, 8 H, $N\mathit{CH_2}Me$, J(HH) 7], 4.89 (s, 3 H, μ-CMe)	358.6 (μ-*C*Me), 222.4, 220.0 (s × 2, WCO), 174.4 (br, $\mathit{C}NCMe_3$), 62.1 (br, *C*Me), 61.6 (br, *C*Me), 58.5 ($CN\mathit{C}Me_3$), 53.0 (br, $N\mathit{CH_2}Me$), 48.8 (μ-C*Me*), 37.7 (br, BCH_2), 34.3 (C*Me*), 32.5 (C*Me*), 32.2 (C*Me*), 30.8 ($CNC\mathit{Me_3}$), 29.8 (C*Me*), 14.8 ($BCH_2\mathit{Me}$), 7.7 ($NCH_2\mathit{Me}$)
14[f]	−5.33 (br, 1 H, B–H→W), 0.57 (s, 3 H, CMe), 0.89 (s, 9 H, $CNCMe_3$), 1.73 (s, 3 H, CMe), 1.74 (s, 3 H, CMe), 1.95 (s, 3 H, CMe), 2.13 (s, 3 H, Me-4), 2.16 (s, 3 H, Me-4), 2.36, 2.50 [(AB), 2 H, BCH_2, J(AB) 14], 4.46 (br, 1 H, NH), 6.96, 7.00 [$(AB)_2$, 4 H, C_6H_4, J(AB) 8], 7.13, 7.97 [$(AB)_2$, 4 H, C_6H_4, J(AB) 8]	218.2, 214.9 (s × 2, WCO), 205.5 [μ-$C(C_6H_4)\mathit{C}N(H)CMe_3$], 150.0 [$\mu$-$\mathit{C}(C_6H_4)CN(H)CMe_3$], 143.2, 139.1 [$C^1(C_6H_4)$], 137.6, 133.1 [$C^4(C_6H_4)$], 131.9, 129.9, 128.7, 128.6 [$C^{2,3}(C_6H_4)$], 71.2 (br, *C*Me), 69.4 (br, *C*Me), 67.2 (br, *C*Me), 65.1 (br, *C*Me), 60.0 ($CN\mathit{C}Me_3$), 32.9 (C*Me*), 31.2 (C*Me*), 30.7 (C*Me*), 29.6 (br, BCH_2), 29.5 (C*Me*), 26.2 (C*Me*), 21.1 (Me-4), 21.0 (Me-4)

[a] Measurements at ambient temperatures in CD_2Cl_2 unless otherwise stated. [b] Hydrogen-1 decoupled, chemical shifts are positive to high frequency of $SiMe_4$. [c] Signal due to B–H→W linkage not observed in ^{1}H spectrum. [d] Measured at 190 K. [e] Measured at 250 K. [f] Measured in C_6D_6.

Table III. Boron-11 NMR Data[a]

compd	^{11}B/δ (J/Hz)
10a	24.5 (1 B, BCH_2), 21.9 (v br, 1 B, B–H→W), 12.3 (2 B, BH), −0.4 (2 B, BH), −2.6 (2 B, BH), −6.9 (8 B, BH), −18.6 (1 B, BH), −28.5 (1 B, BH)
10b	25.9 (1 B, BCH_2), 23.1 (br, 1 B, B–H→W), 11.9 (2 B, BH), −1.4 (2 B, BH), −3.1 (2 B, BH), −6.7 (4 B, BH), −9.5 (2 B, BH), −11.2 (2 B, BH), −19.0 (1 B, BH), −29.6 (1 B, BH)
12a	27.2 (1 B, BCH_2), 18.8 (1 B, B–H→W, J_{BH} 67), +10.0 to −30.1 (16 B, BH)
13a	20.3 (1 B, B–H→W, J_{BH} 67), 13.7 (1 B, BCH_2), +0.1 to −15.6 (16 B, BH)
13b	19.2 (1 B, B–H→W, J_{BH} 73), 14.8 (1 B, BCH_2), −1.1 to −17.6 (16 B, BH)
14	22.2 (1 B, B–H→W, J_{BH} 61), 10.3 (1 B, BCH_2), −4.1 to −12.0 (16 B, BH)

[a] Measurements at ambient temperatures in CD_2Cl_2. Hydrogen-1 decoupled. Chemical shifts (ppm) are positive to high frequency of $BF_3 \cdot Et_2O$ (external).

$[NEt_4][W_2(\mu\text{-}CC_6H_4Me\text{-}4)(CO)_2(\eta^5\text{-}7,8\text{-}Me_2\text{-}7,8\text{-}C_2B_9H_9)\{\eta^6\text{-}7,8\text{-}Me_2\text{-}7,8\text{-}C_2B_9H_8\text{-}10\text{-}(CH_2C_6H_4Me\text{-}4)\}]$ (**10a**).

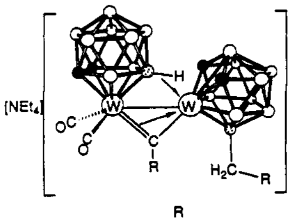

	R
10a	C_6H_4Me-4
10b	Me

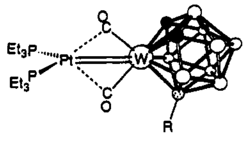

	R
11a	$CH_2C_6H_4Me$-4
11b	CH_2Me
11c	H

● CMe ○ BH ⊗ B

Similarly, the ethylidynetungsten complex **1b** (Y = NEt_4) and 0.5 mol equiv of $HBF_4 \cdot Et_2O$ give $[NEt_4][W_2(\mu\text{-}CMe)(CO)_2(\eta^5\text{-}7,8\text{-}Me_2\text{-}7,8\text{-}C_2B_9H_9)(\eta^6\text{-}7,8\text{-}Me_2\text{-}7,8\text{-}C_2B_9H_8\text{-}10\text{-}Et)]$ (**10b**). The data of characterization for the new salts are given in Tables I–III. However, the structures of these species were not fully established until an X-ray diffraction study on $[NEt_4][W_2(\mu\text{-}CC_6H_4Me\text{-}4)(CO)_2(\eta^5\text{-}7,8\text{-}Me_2\text{-}7,8\text{-}C_2B_9H_9)\{\eta^6\text{-}7,8\text{-}Me_2\text{-}7,8\text{-}C_2B_9H_8\text{-}10\text{-}(CH_2C_6H_4Me\text{-}4)\}]$ (**10a**) had been carried out. The anion of the salt is shown in Figure 1, and important bond lengths and angles are listed in Table IV.

The structure of the anion may be regarded as a dimetallacarborane cluster in which two polyhedral units are connected by tungsten–tungsten, B–H→tungsten and tungsten–carbon–tungsten linkages. Thus, the short W(1)–W(2) vector [2.683 (1) Å] is asymmetrically spanned by a *p*-tolylmethylidyne group [W(1)–C(18) 2.119 (7), W(2)–C(18) 1.999 (7) Å]. One tungsten atom [W(2)] carries two carbonyl ligands and is part of a *closo*-C_2B_9W icosahedron which forms an exopolyhedral B(12)-H(12b)-W(1) linkage to the second tungsten atom. It is the boron atom B(12), situated β to the CMe groups of the CCBBB pentagonal ring ligating W(2), that is involved in this three-center, two-electron bond [W(2)–B(12) 2.31 (1), W(1)–B(12) 2.476 (8) Å]. A striking feature of the structure is the geometry of the other C_2B_9W cage. The C(1)···C(2) separation of 2.917 Å is nonbonding whilst the tungsten atom W(1) is connected to the six atoms C(1), C(2), B(1), B(2), B(3), and B(5), with the two connectivities W(1)–B(2) [2.459 (9) Å] and W(1)–B(5) [2.483 (8) Å] being significantly longer than the four remaining connectivities [W(1)–C(1) 2.041 (6), W(1)–C(2) 2.009 (6), W(1)–B(1) 2.364 (9), W(1)–B(3) 2.349 (7) Å]. As a result of the movement of the atom B(5) toward W(1) the connectivities to its nearest boron neighbors are elongated (1.90–1.93 Å) relative to those (1.74–1.75 Å) for the corresponding atom

Table IV. Selected Internuclear Distances (Å) and Angles (deg) for 10a, with Estimated Standard Deviations in Parentheses

W(1)–W(2)	2.683 (1)	W(1)–C(18)	2.119 (7)	W(2)–C(18)	1.999 (7)	W(1)–B(12)	2.476 (8)
W(1)–H(12b)	1.87	W(2)–C(9)	1.998 (8)	W(2)–C(10)	1.989 (8)	W(1)–C(1)	2.041 (6)
W(1)–C(2)	2.009 (6)	W(1)–B(1)	2.364 (9)	W(1)–B(2)	2.459 (9)	W(1)–B(3)	2.349 (7)
W(1)–B(5)	2.483 (8)	W(2)–C(5)	2.433 (6)	W(2)–C(6)	2.426 (7)	W(2)–B(11)	2.37 (1)
W(2)–B(12)	2.31 (1)	W(2)–B(13)	2.369 (8)	B(12)–H(12b)	1.33	C(1)–B(3)	1.66 (1)
C(1)–B(5)	1.774 (9)	C(1)–B(4)	1.62 (1)	C(2)–B(1)	1.69 (1)	C(2)–B(5)	1.85 (1)
C(2)–B(6)	1.65 (1)	B(1)–B(2)	1.76 (1)	B(1)–B(6)	1.81 (1)	B(1)–B(7)	1.78 (1)
B(2)–B(3)	1.79 (1)	B(2)–B(7)	1.80 (1)	B(2)–B(8)	1.79 (1)	B(3)–B(4)	1.81 (1)
B(3)–B(8)	1.81 (1)	B(4)–B(5)	1.93 (1)	B(4)–B(8)	1.74 (1)	B(4)–B(9)	1.73 (1)
B(5)–B(6)	1.92 (1)	B(5)–B(9)	1.90 (1)	B(6)–B(7)	1.77 (1)	B(6)–B(9)	1.77 (1)
B(7)–B(8)	1.72 (1)	B(7)–B(9)	1.76 (1)	B(8)–B(9)	1.74 (1)	C(5)–C(6)	1.66 (1)
C(5)–B(13)	1.70 (1)	C(5)–B(14)	1.72 (1)	C(5)–B(15)	1.74 (1)	C(6)–B(11)	1.70 (1)
C(6)–B(15)	1.72 (1)	C(6)–B(16)	1.74 (1)	B(11)–B(12)	1.81 (1)	B(11)–B(16)	1.76 (1)
B(11)–B(17)	1.77 (1)	B(12)–B(13)	1.79 (1)	B(12)–B(17)	1.78 (1)	B(12)–B(18)	1.76 (1)
B(13)–B(14)	1.76 (1)	B(13)–B(18)	1.75 (1)	B(14)–B(15)	1.75 (1)	B(14)–B(18)	1.74 (1)
B(14)–B(19)	1.75 (1)	B(15)–B(16)	1.74 (1)	B(15)–B(19)	1.77 (1)	B(16)–B(17)	1.76 (1)
B(16)–B(19)	1.78 (1)	B(17)–B(18)	1.79 (1)	B(17)–B(19)	1.75 (1)	B(18)–B(19)	1.76 (1)
B(2)–C(20)	1.64 (1)	C(20)–C(21)	1.48 (1)	C(9)–O(9)	1.15 (1)	C(10)–O(10)	1.14 (1)

W(1)–W(2)–C(18)	51.3 (2)	W(2)–W(1)–C(18)	47.4 (2)	W(1)–C(18)–W(2)	81.3 (3)
W(1)–C(18)–C(11)	137.3 (5)	W(2)–C(18)–C(11)	140.5 (5)	W(2)–C(9)–O(9)	178.0 (6)
W(2)–C(10)–O(10)	176.9 (7)	B(2)–C(20)–C(21)	113.7 (5)	W(1)–H(12b)–B(12)	99.9 (2)
W(1)–B(12)–H(12b)	48.2 (2)				

B(15) in the *closo*-$C_2B_9W(2)$ icosahedron. The atom B(2) which is in a site β to the two carbon atoms of the CBCBBB ring adjacent to the metal vertex carries a $CH_2C_6H_4Me$-4 substituent.

In the solid state the anion as a whole does not possess a plane of symmetry. However, the atoms W(1), H(12b), B(12), W(2) and C(18) are essentially coplanar with B(5) lying slightly out of this plane (0.267 Å). This approximate plane of symmetry is important in the discussion of the NMR data of **10a** and **10b** (below).

The distorted icosahedral topology of the $C_2B_9W(1)$ fragment in **10a** is identical with that previously described in the complex $[PtW(CO)_2(PEt_3)_2\{\eta^6\text{-}7,8\text{-}Me_2\text{-}7,8\text{-}C_2B_9H_8\text{-}10\text{-}(CH_2C_6H_4Me\text{-}4)\}]$ (**11a**).[6] Assuming that the metal atom W(1) and its associated ligand set contributes three orbitals and zero electrons [W(0) d^6] to cluster bonding then the $W(1)C_2B_9H_8(CH_2C_6H_4Me\text{-}4)$ fragment should be regarded as a 12-vertex cluster with only 12 skeletal electron pairs. Geometrically distorted polyhedral structures of this type (*n* vertices with fewer than $n + 1$ skeletal electron pairs) have been termed hyper-closo.[7,8] An alternative description of this bonding utilizing the iso-closo model of Kennedy[9,10] would give a 12-vertex cluster with 13 skeletal electron pairs. However, a theoretical comparison of these two models, for an idealized 10-vertex system, favored the description hyper-closo,[11] which we prefer for the complexes described herein.

Once the structure of **10a** is determined, the spectroscopic data for both **10a** and **10b** can be interpreted. Thus, the $^{11}B\{^1H\}$ NMR spectra (Table III) each show two deshielded resonances due to the BCH_2R and the B–H→W nuclei.[6] Although neither signal becomes a doublet in a proton-coupled spectrum, the less deshielded peak in each case is considerably broader due to unresolved HB coupling and is therefore assigned to the boron atom of the B–H→W linkage. In the ^1H NMR spectrum of **10a** the $BCH_2C_6H_4Me$-4 protons give rise to a broad signal at δ 2.82 ppm whilst the five protons of the BCH_2CH_3 group of **10b** are seen as a triplet (CH_3) and a quartet (CH_2) at δ 0.68 and 1.40 ppm, respectively. Signals associated with the B–H→W linkages are not observed in the ^1H NMR spectrum of either species, presumably a consequence of unfavorable relaxation due to the quadrupolar ^{11}B nuclei.

Resonances arising from the carbonyl ligands and the metallacarborane moieties imply that on the NMR time scale the anions of both **10a** and **10b** possess a plane of symmetry defined by the atoms B(2), B(5), W(1), C(18), W(2), and B(12), even at temperatures as low as ca. 190 K. Thus, in the ^1H and $^{13}C\{^1H\}$ spectra the two CMe groups of each cage appear equivalent throughout the temperature range 190–295 K, though the signals are substantially broader at the highest temperature studied. Similarly, in the $^{13}C\{^1H\}$ spectrum at 190 K one sharp resonance is seen for the two carbonyl groups (Table II) but this also becomes increasingly broad as the temperature is raised. These observations are consistent with two fluxional processes which afford the anions a time-averaged plane of symmetry. The appearance of equivalent CMe groups for each cage even at the lowest temperature studied implies that the two C_2B_9 moieties are rocking back and forth across the plane defined by W(1), W(2), and C(18) so that on the NMR time scale the atoms B(2), B(5), and B(12) lie in this plane with the two pairs of CMe groups lying on either side and equidistant from it. This coupled with slow rotation of the μ-CC_6H_4Me-4 fragment about C(11)–C(18) would lead to the observations described above. That the resonances become sharp at 190 K suggest that the latter process does not occur at this temperature and that the μ-*p*-tolyl ring adopts an orientation perpendicular to the W–W vector so as not to destroy the time-averaged symmetry.

Resonances at ca. δ 180 ppm in the $^{13}C\{^1H\}$ NMR spectra are ascribed to the CMe nuclei of the η^6-7,8-C_2B_9W moieties. Although this is extremely high frequency for cage carbon atoms in a 12-vertex polyhedron the values are in excellent agreement with those observed for compounds **11** (δ 176.6–180.1 ppm)[6] and would appear to be diagnostic of this hyper-closo cage structure. In accord with these species being electronically unsaturated dimetal complexes (32 valence electrons), the bridging alkylidyne groups give rise to relatively deshielded signals at δ 346.7 (**10a**) and 343.6 ppm (**10b**) due to the μ-C nuclei.[12]

---

[6] Attfield, M. J.; Howard, J. A. K.; Jelfs, A. N. de M.; Nunn, C. M.; Stone, F. G. A. *J. Chem. Soc., Dalton Trans.* **1987**, 2219.

[7] Baker, R. T. *Inorg. Chem.* **1986**, *25*, 109.

[8] (a) Jung, C. W.; Baker, R. T.; Knobler, C. B.; Harthorne, M. F. *J. Am. Chem. Soc.* **1980**, *102*, 5782. (b) Jung, C. W.; Baker, R. T.; Hawthorne, M. F. *J. Am. Chem. Soc.* **1981**, *103*, 810.

[9] Kennedy, J. D. *Inorg. Chem.* **1986**, *25*, 111.

[10] (a) Greenwood, N. N. *Chem. Soc. Rev.* **1984**, *13*, 353. (b) Greenwood, N. N. *Pure Appl. Chem.* **1983**, *55*, 77. (c) Crook, J. E.; Erlington, M.; Greenwood, N. N.; Kennedy, J. D.; Woolins, J. D. *Polyhedron* **1984**, *3*, 901. (d) Crook, J. E.; Erlington, M.; Greenwood, N. N.; Kennedy, J. D.; Thornton-Pett, M.; Woolins, J. D. *J. Chem. Soc., Dalton Trans.* **1985**, 2407.

[11] Johnston, R. L.; Mingos, D. M. P. *Inorg. Chem.* **1986**, *25*, 3321.

Scheme I. Key: (i) $HBF_4 \bullet Et_2O$, -78 °C; (ii) $[NEt_4][W(\equiv CR)(CO)_2(\eta^5\text{-}7,8\text{-}Me_2\text{-}7,8\text{-}C_2B_9H_9)]$

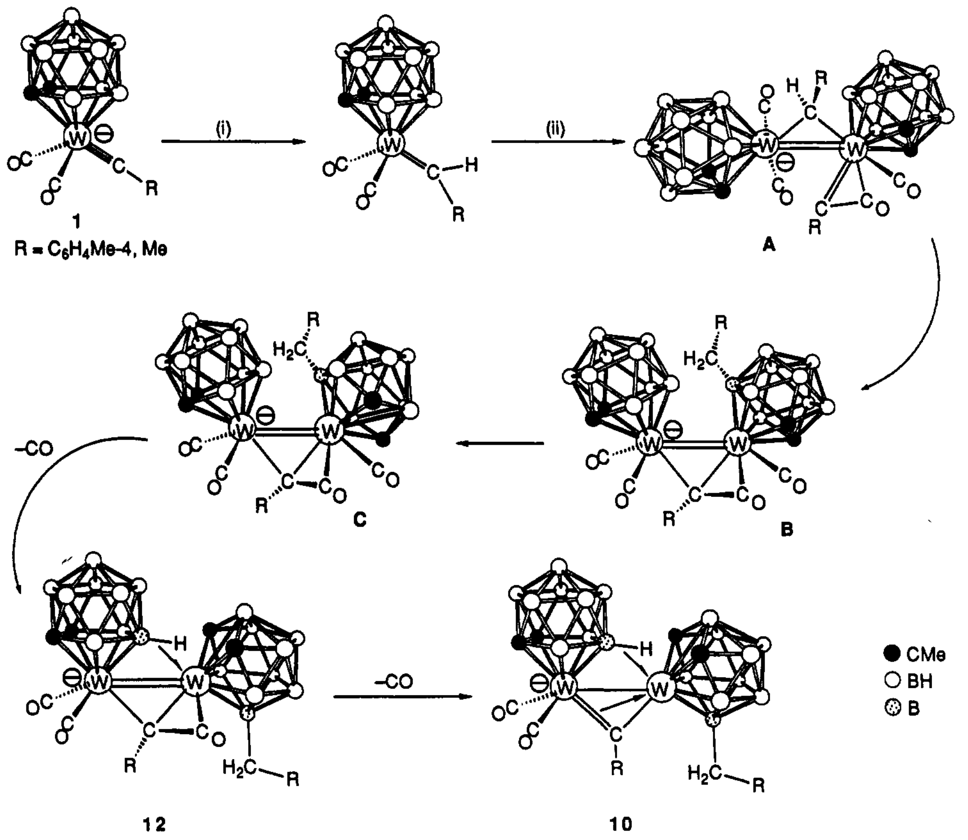

During the synthesis of **10a** it was noticed that if the reaction was "worked-up" at temperatures at or below 0 °C, then column chromatography yielded an additional fraction. Low-temperature NMR measurements showed this fraction to be composed initially of trace levels (<5%) of **10a**, $[NEt_4][\textit{nido}\text{-}7,8\text{-}Me_2\text{-}7,8\text{-}C_2B_9H_{10}]$,[13] and a third species characterized as the ketenyl complex $[NEt_4][W_2\{\mu\text{-}\eta^2\text{-}C(C_6H_4Me\text{-}4)CO\}(CO)_2(\eta^5\text{-}7,8\text{-}Me_2\text{-}7,8\text{-}C_2B_9H_9)\{\eta^6\text{-}7,8\text{-}Me_2\text{-}7,8\text{-}C_2B_9H_8\text{-}10\text{-}(CH_2C_6H_4Me\text{-}4)\}]$ (**12a**). The presence of the ketenyl group in **12a** is apparent from both the IR spectrum (Table I) which shows a RCCO stretch at 1753 cm^{-1} and the $^{13}C\{^1H\}$ NMR spectrum (Table II) in which signals at δ 187.5 and 94.8 ppm can be assigned to the $C(C_6H_4Me\text{-}4)CO$ and $\textit{C}(C_6H_4Me\text{-}4)CO$ nuclei, respectively. These values fall in the region midway between the ranges generally found for μ-η^1 and μ-η^2 attachment of a ketenyl ligand at a dimetal center[14-16] and are probably best interpreted as indicating a bonding mode that is intermediate between the two forms

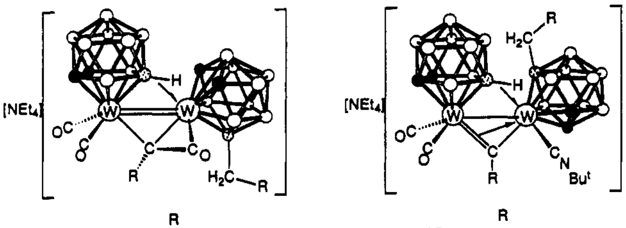

	R			R
12a	C_6H_4Me-4		**13a**	C_6H_4Me-4
12b	Me		**13b**	Me

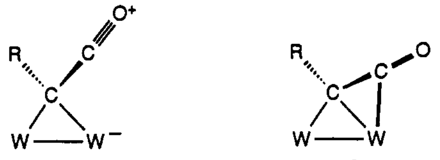

μ-η^1 μ-η^2

The remaining spectroscopic data for **12a** are entirely consistent with the proposed structure. Thus, the pairs of resonances at δ 184.4 and 176.5 and at δ 69.2 and 67.8 ppm in the $^{13}C\{^1H\}$ NMR spectrum are due to the CMe atoms of the $\eta^6\text{-}7,8\text{-}C_2B_9W$ (hyper-closo) and the $\eta^5\text{-}7,8\text{-}C_2B_9W$ (closo) metallacarborane cage, respectively, whilst the BCH_2 protons appear as an [AB] pattern in the ^1H NMR spectrum. Although the presence of the B–H→W bond is not apparent in the ^1H spectrum, a diagnostic doublet resonance at δ 18.8 ppm (*J* = 67 Hz) is observed in the proton-coupled ^{11}B NMR spectrum. Moreover, a singlet at δ 27.2 ppm in the $^{11}B\{^1H\}$ spectrum arises from the boron vertex carrying the $CH_2C_6H_4Me\text{-}4$ substituent (Table III). It is interesting to compare the ^{11}B chemical shifts of the BCH_2R groups present in these 12-vertex hyper-closo cages with those found in corresponding closo systems. In general, the latter are observed at δ <10 ppm[2-4] whereas values in excess of 25 ppm are found for all the compounds **10**, **11**, and **12a**. The origin of this additional deshielding is unknown, but must be associated with the distorted cage geometry observed in these species.

It was observed that solutions of **12a** slowly convert to **10a** by the loss of a molecule of CO, conversion being complete in ca. 4 h at 25 °C. Consequently, **12a** could not be isolated free of **10a**. Compound **12b**, analogous to **12a**, which may have resulted from protonation of **1b** (Y = NEt_4), was not observed during the synthesis of **10b**,

---

[12] Dossett, S. J.; Hart, I. J.; Stone, F. G. A. *J. Chem. Soc., Dalton Trans.* **1990**, 3481 and references cited therein.

[13] Hawthrone, M. F.; Young, D. C.; Garrett, P. M.; Owen, D. A.; Schwerin, S. G.; Tebbe, F. N.; Wegner, P. A. *J. Am. Chem. Soc.* **1968**, *90*, 862.

[14] Geoffroy, G. L.; Bassner, S. L. *Adv. Organomet. Chem.* **1988**, *28*, 1.

[15] Jeffery, J. C.; Sambale, C.; Schmidt, M. F.; Stone, F. G. A. *Organometallics* **1982**, *1*, 1597.

[16] Jeffery, J. C.; Ruiz, M. A.; Stone, F. G. A. *J. Organomet. Chem.* 1988, *355*, 231.

presumably due to its thermal instability.

The mode of formation of these species is essentially unknown, but protonation would initially give the alkylidene species $[W\{=C(H)R\}(CO)_2(\eta^5\text{-}7,8\text{-}Me_2\text{-}7,8\text{-}C_2B_9H_9)]$ which could readily complex with the anion $[W(\equiv CR)(CO)_2(\eta^5\text{-}7,8\text{-}Me_2\text{-}7,8\text{-}C_2B_9H_9)]^-$, possibly to give an anionic η^2-ketenyl complex (**A** in Scheme I). In this respect we have previously shown[5] that **1a** [Y = $N(PPh_3)_2$] reacts with strong nucleophiles (e.g. L = PMe_3) to afford the η^2-ketenyl complexes $[N(PPh_3)_2][W(CO)(L)\{\eta^2\text{-}C(C_6H_4Me\text{-}4)CO\}(\eta^5\text{-}7,8\text{-}Me_2\text{-}7,8\text{-}C_2B_9H_9)]$. For the pathway invoked herein the nucleophile (L) would be the alkylidene species. Migration and insertion of the μ-C(H)R group into a B—H bond accompanied by formation of a μ-η^2-ketenyl ligand could then give an intermediate binuclear species **B** in which one of the metal centers is electron deficient (16 valence electrons). That tungsten strongly prefers to form 18- rather than 16-electron organocomplexes may then be the driving force necessary to bring about the closo to hyper-closo transformation present in **C**. By this means the electron deficiency of the hyper-closo cage is more evenly distributed amongst its constituent atoms and the tungsten vertex thereby receives a greater share of the available electrons. Formation of a B—H→W bond via displacement of a CO ligand would then give the species **12**, which as described above subsequently releases a molecule of CO to afford the products **10**.

As mentioned earlier, the salts **10** are formally unsaturated species which might therefore be expected to react with donor molecules in a manner paralleling that observed for the hyper-closo metallacarboranes $[PtW(CO)_2(PEt_3)_2\{\eta^6\text{-}7,8\text{-}Me_2\text{-}7,8\text{-}C_2B_9H_8\text{-}10\text{-}(CH_2C_6H_4Me\text{-}4)\}]$ (**11a**)[6] and $[Ru(PPh_3)_2(\eta^6\text{-}5,6\text{-}C_2B_7H_7)]$.[8] Both of these compounds add donor molecules to give species containing closo 12- and 10-vertex cage clusters, respectively.

Treatment of **10a** or **10b** with $CNBu^t$ affords the brown salts $[NEt_4][W_2(\mu\text{-}CR)(CNBu^t)(CO)_2(\eta^5\text{-}7,8\text{-}Me_2\text{-}7,8\text{-}C_2B_9H_9)\{\eta^5\text{-}7,8\text{-}Me_2\text{-}7,8\text{-}C_2B_9H_8\text{-}10\text{-}(CH_2R)\}]$ (R = C_6H_4Me-4 (**13a**); R = Me (**13b**)), in which the electronic unsaturation of the *hyper-closo*-C_2B_9W fragment in the parent compound has been relieved and a closo cage regenerated. The spectroscopic data for **13a** and **13b** are given in Tables I–III. The presence of a terminally bound isocyanide ligand in each product is evident from the observation of a C≡N stretching band at 2110 (**13a**) and 2109 cm^{-1} (**13b**) in the infrared spectrum as well as signals due to the $CNBu^t$ nucleus at δ 161.6 (**13a**) and 174.4 ppm (**13b**) in the $^{13}C\{^1H\}$ NMR spectrum.[17] The fact that a closo cage has been regenerated is demonstrated by the nonappearance of signals due to the cage *C*Me atoms in the region ca. δ 180 ppm, as discussed above. However, the observation of only two such signals (δ ca. 62 ppm) rather than the expected four must be due to coincidence since the anions clearly do not possess a plane of symmetry. Furthermore, four resonances are observed in both the ^1H and $^{13}C\{^1H\}$ spectra for the C*Me* groups. The remainder of the spectroscopic data are as expected.

Protonation of **13a** with $HBF_4 \cdot Et_2O$ in CH_2Cl_2 yielded a deep blue species which on the basis of spectroscopic data we formulate as the electronically unsaturated (30 c.v.e.) complex $[W_2\{\mu\text{-}C(C_6H_4Me\text{-}4)CN(H)Bu^t\}(CO)_2(\eta^5\text{-}7,8\text{-}Me_2\text{-}7,8\text{-}C_2B_9H_9)\{\eta^5\text{-}7,8\text{-}Me_2\text{-}7,8\text{-}C_2B_9H_8\text{-}10\text{-}(CH_2C_6H_4Me\text{-}4)\}]$ (**14**). Thus, the $^{11}B\{^1H\}$ NMR spectrum shows two deshielded resonances at δ 22.2 and 10.3 ppm. Since the former of these becomes a doublet (*J* = 61 Hz) in a proton-coupled spectrum whilst the latter remains a singlet, these are ascribed to B–H→W and B–$CH_2C_6H_4Me$-4 linkages, respectively. In accord with this assignment, the ^1H NMR spectrum shows a broad unresolved multiplet at δ −5.33 ppm due to the B–H→W proton and an [AB] spin pattern at δ 2.36 and 2.50 ppm (*J* = 14 Hz) arising from the BCH_2 protons. In addition, a relatively broad signal at δ 4.46 ppm, and integrating for one proton, is assigned to the NH group.

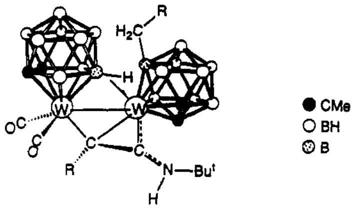

14 R = C_6H_4Me-4

The $^{13}C\{^1H\}$ NMR spectrum of **14** confirms the presence of the $BCH_2C_6H_4Me$-4 nucleus by the appearance of a broad multiplet at δ 29.6 ppm, whilst the observation of four signals at δ 71.2, 69.4, 67.2, and 65.1 ppm due to the cage *C*Me nuclei are consistent with two *closo*-7.8-C_2B_9W cages. Resonances associated with the two ligated carbon atoms of the μ-$C(C_6H_4Me\text{-}4)CN(H)Bu^t$ ligand occur at δ 205.5 and 150.0 ppm. These values should be compared with those for the corresponding signals in the spectrum of the compound $[WCo(O)\{\mu\text{-}C(C_6H_4Me\text{-}4)C(OMe)\}(\mu\text{-}PPh_2)(CO)(PPh_2H)(\eta\text{-}C_5H_5)][BF_4]$ for which an X-ray structural analysis showed that the μ-alkyne ligand adopts a novel asymmetric mode of attachment.[18] In the latter species the ligated alkyne carbon atom carrying the *p*-tolyl substituent (δ 230 ppm) bridges the W–Co bond whilst the methoxy-bearing carbon atom (δ 126.6–139.6 ppm; the precise chemical shift is unknown due to the plethora of signals in this region due to the Ph and *p*-tolyl groups) is bound only to the Co center. In view of the similarity in chemical shift data for the two compounds $[WCo(O)\{\mu\text{-}C(C_6H_4Me\text{-}4)C(OMe)\}(\mu\text{-}PPh_2)(CO)(PPh_2H)(\eta\text{-}C_5H_5)][BF_4]$ and **14** it seems reasonable to propose that they have similar structures with respect to the bonding of the alkyne ligand, so that for **14** the carbon atom carrying the *p*-tolyl group (δ 150.0 ppm) is bound to both metal centers whilst the *C*N(H)Bu^t carbon (δ 205.5 ppm) is linked only to one.

This type of bonding, in which the alkyne is twisted with respect to the metal–metal vector has been observed in several other complexes in which one of the ligated carbon atoms of the alkyne carries a heteroatom substituent. It is intermediate between the commonly observed transverse and in-plane bonding modes of alkyne molecules at dimetal centers.[19] In particular the μ-$C(Me)CNEt_2$ ligand in the complexes $[Fe_2\{\mu\text{-}C(Me)CNEt_2\}(CO)_7]$[19d] and $[FeRu\{\mu\text{-}C(Me)CNEt_2\}(CO)_5(L)]$ (L = Pr^i—N=CHC(H)=NPr^i)[19e] is bound in the same manner with electron density delocalized over the M—C—N fragment. The observation of a CN stretching vibration at 1596 cm^{-1} for **14** implies a degree of multiple bond character suggestive of similar delocalization of electron density over the W—C—N moiety.

Formation of **14** via protonation of **13a** is readily rationalized; protonation at the isocyanide N atom could

---

(17) Cronin, D. L.; Wilkinson, J. R.; Todd, L. J. *J. Magn. Reson.* **1975**, *17*, 353.

(18) El Amin, E.; Jeffery, J. C.; Walters, T. M. *J. Chem. Soc., Chem. Commun.* **1990**, 170.

(19) (a) Adams, R. D.; Chen, G.; Tanner, J. T.; Yin, J. *Organometallics* **1990**, *9*, 595. (b) Adams, R. D.; Tanner, J. T. *Organometallics* **1989**, *8*, 563. (c) Templeton, J. L. *Adv. Organomet. Chem.* **1989**, *29*, 1. (d) Muller, F.; Van Koten, G.; Kraakman, M. J. A.; Vrieze, K.; Heijdenrijk, D.; Zoutberg, M. C. *Organometallics* **1989**, *8*, 1331. (e) Cabrera, E.; Daran, J.-C.; Jeannin, Y.; Kristiansson, O. *J. Organomet. Chem.* **1986**, *310*, 367. (f) Brew, S. A.; Dossett, S. J.; Jeffery, J. C.; Stone, F. G. A. *J. Chem. Soc., Dalton Trans.* **1990**, 3709.

Table V. Crystallographic Data for 10a[a]

cryst dimens/mm	0.51 × 0.16 × 0.16
formula	$C_{34}H_{65}B_{18}NO_2W_2$
M_r	1082.2
cryst color, shape	orange prisms
cryst syst	monoclinic
space group	$P2_1/n$ (No. 14)
a/Å	15.4967 (8)
b/Å	21.2541 (7)
c/Å	15.7528 (9)
β/deg	118.276 (5)
V/Å^3	4561.1 (4)
Z	4
d_{calcd}/g cm^{-3}	1.576
μ(Mo Kα)/cm^{-1}	51.8
F(000)/e	2120
2θ range/deg	3–40
T/K	292
no. of reflns measd	4627
no. of unique reflns	4251
no. of obs reflns	3744
criterion for observed n [$F_o \geq n\sigma(F_o)$]	$n = 4$
R (R')[b]	0.0212 (0.0239)
final electron density diff features (max/min)/e Å^{-3}	0.55/−0.55
S (goodness-of-fit)	1.3

[a] Data collected on an Enraf-Nonius CAD4-F automated diffractometer operating in the ω–2θ scan mode (h, 0–14; k, 0–20; l −15 to +13); graphite-monochromated Mo Kα X-radiation, $\bar{\lambda}$ = 0.710 73 Å. Refinement was by block full-matrix least-squares on F with a weighting scheme of the form $w^{-1} = [\sigma^2(F_o) + 0.00029|F_o|^2]$ where $\sigma_c^2(F_o)$ is the variance in F_o due to counting statistics. [b] $R = \sum||F_o| - |F_c||/\sum|F_o|$, $R' = \sum w^{1/2}||F_o| - |F_c||/\sum w^{1/2}|F_o|$.

Table VI. Atomic Coordinates (×10^4) and Equivalent Isotropic Displacement Parameters (Å^2 × 10^3) for 10a

name	x	y	z	U(eq)[a]
W(1)	2184 (1)	2138 (1)	977 (1)	32 (1)
W(2)	2104 (1)	3284 (1)	1652 (1)	34 (1)
C(9)	2274 (5)	3489 (3)	2960 (5)	54 (2)
O(9)	2365 (5)	3589 (3)	3716 (4)	91 (2)
C(10)	657 (5)	3287 (3)	1124 (5)	52 (2)
O(10)	−177 (4)	3276 (3)	785 (4)	79 (2)
C(11)	1874 (4)	2156 (3)	2943 (4)	37 (2)
C(12)	2498 (5)	1718 (3)	3616 (4)	47 (2)
C(13)	2242 (5)	1441 (3)	4254 (4)	54 (2)
C(14)	1363 (5)	1557 (3)	4246 (4)	48 (2)
C(15)	765 (5)	2010 (3)	3604 (5)	48 (2)
C(16)	1015 (5)	2311 (3)	2984 (4)	44 (2)
C(17)	1049 (5)	1180 (3)	4883 (5)	68 (2)
C(18)	2070 (4)	2442 (3)	2201 (4)	38 (2)
C(1)	1152 (4)	1462 (3)	716 (4)	40 (2)
C(2)	3285 (4)	1543 (3)	1760 (4)	47 (2)
B(1)	3358 (5)	1575 (4)	725 (5)	44 (2)
B(2)	2247 (6)	1586 (4)	−364 (5)	44 (2)
B(3)	1102 (5)	1533 (4)	−352 (5)	44 (2)
B(4)	1145 (6)	791 (3)	231 (6)	53 (2)
B(5)	2219 (5)	1022 (4)	1460 (6)	49 (2)
B(6)	3366 (6)	850 (4)	1333 (6)	57 (3)
B(7)	2920 (6)	862 (4)	71 (6)	55 (2)
B(8)	1660 (6)	835 (3)	−540 (6)	52 (2)
B(9)	2273 (6)	451 (4)	562 (6)	59 (3)
C(3)	281 (4)	1532 (3)	912 (5)	56 (2)
C(4)	4151 (5)	1677 (3)	2742 (4)	56 (2)
C(20)	2190 (5)	1934 (3)	−1323 (4)	49 (2)
C(21)	2816 (5)	1637 (3)	−1684 (4)	43 (2)
C(22)	3776 (5)	1823 (3)	−1358 (5)	57 (2)
C(23)	4376 (5)	1510 (3)	−1656 (5)	58 (2)
C(24)	4036 (5)	1013 (3)	−2296 (5)	57 (2)
C(25)	3084 (5)	844 (3)	−2651 (5)	52 (2)
C(26)	2490 (5)	1151 (3)	−2348 (4)	51 (2)
C(27)	4713 (6)	674 (4)	−2589 (6)	85 (3)
C(5)	2154 (4)	4324 (3)	1033 (4)	42 (2)
C(6)	3275 (4)	4095 (3)	1815 (4)	43 (2)
B(11)	3542 (5)	3387 (3)	1496 (6)	46 (2)
B(12)	2462 (5)	3162 (4)	399 (5)	41 (2)
B(13)	1592 (6)	3780 (4)	142 (5)	47 (2)
B(14)	2101 (6)	4469 (4)	−64 (6)	56 (2)
B(15)	3151 (6)	4670 (4)	998 (6)	58 (3)
B(16)	4017 (6)	4079 (4)	1264 (6)	59 (3)
B(17)	3501 (6)	3498 (4)	365 (6)	57 (3)
B(18)	2287 (6)	3745 (4)	−466 (6)	56 (2)
B(19)	3248 (7)	4293 (4)	43 (6)	63 (3)
C(7)	3772 (5)	4359 (3)	2839 (4)	60 (2)
C(8)	1592 (5)	4792 (3)	1332 (5)	55 (2)
N	2219 (4)	3543 (3)	6437 (4)	52 (2)
C(91)	1470 (6)	4035 (4)	5875 (6)	91 (3)
C(92)	1006 (7)	4369 (5)	6382 (8)	126 (3)
C(93)	3074 (5)	3829 (4)	7314 (5)	70 (2)
C(94)	3599 (7)	4347 (4)	7114 (7)	113 (3)
C(95)	2553 (6)	3266 (4)	5756 (5)	72 (3)
C(96)	3251 (6)	2720 (4)	6161 (6)	90 (3)
C(97)	1797 (5)	3050 (4)	6816 (5)	61 (2)
C(98)	972 (5)	2674 (4)	6064 (5)	80 (3)

[a] Equivalent isotropic U defined as one-third of the trace of the orthogonalized U_{ij} tensor.

generate an aminocarbyne M≡C—N(H)Bu^t moiety[20] adjacent to the μ-p-tolylmethylidyne group. Coupling of the carbyne ligands would then give the observed product.

Conclusions

The new metallacarborane complexes presented here and elsewhere[2-4] contrast sharply with those obtained from protonation of the analogous compounds $[N(PPh_3)_2][W(\equiv CR)(CO)_2(\eta^5\text{-}7,8\text{-}C_2B_9H_{11})]$, containing unsubstituted carborane cages.[5] The difference in reactivity appears to stem from the reluctance of the latter type of complex to undergo intramolecular migration and insertion of organic fragments into cage B—H bonds, a feature which is prevalent in the chemistry of species containing C-methyl-substituted carborane cages. Metallacarboranes having the cage topology identified in the salt **10a** are extremely rare[6,8] and deserving of further study, both from a chemical and a theoretical viewpoint, since neither the reasons for their formation nor the electronic properties of such clusters are entirely understood.

Experimental Section

General. All reactions were carried out under an atmosphere of dry nitrogen using Schlenk-line techniques. Solvents were distilled from appropriate drying agents under nitrogen before use. Petroleum ether refers to that fraction of bp 40–60 °C. Chromatography columns (ca. 15 cm in length and 2 cm in diameter) were packed with either alumina (Brockmann activity II) or silica gel (Aldrich, 70–230 mesh). The compounds $[NEt_4][W(\equiv CC_6H_4Me\text{-}4)(CO)_2(\eta^5\text{-}7,8\text{-}Me_2\text{-}7,8\text{-}C_2B_9H_9)]$ (**1a**)[21] and $[NEt_4][W(\equiv CMe)(CO)_2(\eta^5\text{-}7,8\text{-}Me_2\text{-}7,8\text{-}C_2B_9H_9)]$ (**1b**)[3] were prepared as previously described. The acid $HBF_4{\cdot}Et_2O$ was used as purchased from Aldrich Chemical Co. as an 85% solution in Et_2O.

Instrumentation. NMR spectra were recorded at ambient temperatures, unless otherwise stated, using a Bruker AMX 360 spectrometer. The chemical shifts for ^1H and $^{13}C\{^1H\}$ spectra are referenced to $SiMe_4$, and those for the ^{11}B spectra, measured in CD_2Cl_2, are positive to high frequency of $BF_3{\cdot}Et_2O$ (external). IR spectra were measured with a Bruker IFS 25 FT-IR spectrometer.

Protonation of the Salts $[NEt_4][W(\equiv CR)(CO)_2(\eta^5\text{-}7,8\text{-}Me_2\text{-}7,8\text{-}C_2B_9H_9)]$ (R = Me or C_6H_4Me-4). (i) A rapidly stirred solution of $[NEt_4][W(\equiv CC_6H_4Me\text{-}4)(CO)_2(\eta^5\text{-}7,8\text{-}Me_2\text{-}7,8\text{-}C_2B_9H_9)]$ (**1a**) (0.23 g, 0.36 mmol) in CH_2Cl_2 (20 mL) was cooled to ca. −78 °C and treated with $HBF_4{\cdot}Et_2O$ (25 μL, 0.16 mmol). The resulting solution was allowed to warm to ca. 0 °C, the solvent was reduced in volume in vacuo to ca. 5 mL, and the solution was chromatographed on alumina at ca −20 °C. Elution with CH_2Cl_2 first removed a trace of $[W(CO)_4\{\eta^5\text{-}7,8\text{-}Me_2\text{-}7,8\text{-}C_2B_9H_8\text{-}10\text{-}$

---

(20) Chatt, J.; Pombeiro, A. J. L.; Richards, R. L.; Royston, G. H. D.; Muir, K. W.; Walker, R. *J. Chem. Soc., Chem. Commun.* **1975**, 708.

(21) Baumann, F. E.; Howard, J. A. K.; Johnson, O.; Stone, F. G. A. *J. Chem. Soc., Dalton Trans.* **1987**, 2661.

(CH$_2$C$_6$H$_4$Me-4)}] (**5a**) (identified by IR spectroscopy)[4] followed by an orange eluate. Further elution with CH$_2$Cl$_2$–THF (4:1) removed a red fraction. The volume of the orange solution was reduced in vacuo to ca. 2 mL and petroleum ether allowed to slowly diffuse into this solution to yield orange *crystals* of [NEt$_4$][W$_2$(μ-CC$_6$H$_4$Me-4)(CO)$_2$(η^5-7,8-Me$_2$-7,8-C$_2$B$_9$H$_9$){η^6-7,8-Me$_2$-7,8-C$_2$B$_9$H$_8$-10-(CH$_2$C$_6$H$_4$Me-4)}] (**10a**) (0.06 g). Anal. Calcd for C$_{34}$H$_{65}$NB$_{18}$O$_2$W$_2$: C, 37.74; H, 6.05; N, 1.29. Found: C, 37.05; H, 6.48; N, 1.31. NMR measurements on the red solution showed it to be a mixture of **10a**, [NEt$_4$][W$_2${μ-η^2-C(C$_6$H$_4$Me-4)CO}-(CO)$_2$(η^5-7,8-Me$_2$-7,8-C$_2$B$_9$H$_9$){η^6-7,8-Me$_2$-7,8-C$_2$B$_9$H$_8$-10-(CH$_2$C$_6$H$_4$Me-4)}] (**12a**), and [NEt$_4$][*nido*-7,8-Me$_2$-7,8-C$_2$B$_9$H$_{10}$]. Analytically pure samples of **12a** could not be obtained due to its thermal instability. Thus, NMR measurements on these solutions showed that **12a** decomposed cleanly to **10a** in a period of ca. 4 h at 25 °C. Column chromatography of the resulting solutions on alumina, eluting with CH$_2$Cl$_2$, led to isolation of **10a** only.

(ii) Similarly, [NEt$_4$][W($\equiv$CMe)(CO)$_2$(η^5-7,8-Me$_2$-7,8-Me$_2$-7,8-C$_2$B$_9$H$_9$)] (**1b**) (0.26 g, 0.47 mmol) and HBF$_4$·Et$_2$O (29 μL, 0.19 mmol) in CH$_2$Cl$_2$ (20 mL) gave a trace of [W(CO)$_4$(η^5-7,8-Me$_2$-7,8-C$_2$B$_9$H$_8$-10-Et)] (**5b**) (identified by IR spectroscopy)[4] and orange *microcrystals* of [NEt$_4$][W$_2$(μ-CMe)(CO)$_2$(η^5-7,8-Me$_2$-7,8-C$_2$B$_9$H$_9$)(η^6-7,8-Me$_2$-7,8-C$_2$B$_9$H$_8$-10-Et)] (**10b**) (0.07 g). Anal. Calcd for C$_{22}$H$_{57}$NB$_{18}$O$_2$W$_2$: C, 28.41; H, 6.18; N, 1.51. Found: C, 28.02; H, 6.32; N, 1.57. All attempts to isolate a compound **12b**, analogous to **12a**, were unsuccessful, giving a mixture comprised mainly of **10b** and [NEt$_4$][*nido*-7,8-Me$_2$-7,8-C$_2$B$_9$H$_{10}$).

Reactions with CNBu^t. (i) To a solution of [NEt$_4$][W$_2$(μ-CC$_6$H$_4$Me-4)(CO)$_2$(η^5-7,8-Me$_2$-7,8-C$_2$B$_9$H$_9$){η^6-7,8-Me$_2$-7,8-C$_2$B$_9$H$_8$-10-(CH$_2$C$_6$H$_4$Me-4)}] (**10a**) (0.30 g, 0.28 mmol) in CH$_2$Cl$_2$ (15 mL) was added CNBu^t (35 μL, 0.31 mmol), and the resulting brown solution was stirred for 2 h. The volume of solvent was reduced in volume in vacuo to ca. 4 mL and the solution chromatographed on alumina. Elution with CH$_2$Cl$_2$ gave a brown solution which upon concentration to ca. 5 mL and addition of *n*-hexane (20 mL) gave brown *microcrystals* of [NEt$_4$][W$_2$(μ-CC$_6$H$_4$Me-4)(CNBu^t)(CO)$_2$(η^5-7,8-Me$_2$-7,8-C$_2$B$_9$H$_9$){η^5-7,8-Me$_2$-7,8-C$_2$B$_9$H$_8$-10-(CH$_2$C$_6$H$_4$Me-4)}] (**13a**) (0.29 g). Anal. Calcd for C$_{39}$H$_{74}$N$_2$B$_{18}$O$_2$W$_2$: C, 40.20; H, 6.40; N, 2.40. Found: C, 39.68; H, 7.32; N, 2.16.

(ii) To a CH$_2$Cl$_2$ (15 mL) solution of [NEt$_4$][W$_2$(μ-CMe)-(CO)$_2$(η^5-7,8-Me$_2$-7,8-C$_2$B$_9$H$_9$)(η^6-7,8-Me$_2$-7,8-C$_2$B$_9$H$_8$-10-Et)] (**10b**) (0.15 g, 0.16 mmol) was added CNBu^t (18 μL, 0.16 mmol) to give a brown solution which after 2 h was concentrated in vacuo to ca. 5 mL and chromatographed on alumina. Elution with CH$_2$Cl$_2$ gave a brown eluate which upon concentration in vacuo to ca. 5 mL and addition of petroleum ether (20 mL) gave brown *microcrystals* of [NEt$_4$][W$_2$(μ-CMe)(CNBu^t)(CO)$_2$(η^5-7,8-Me$_2$-7,8-C$_2$B$_9$H$_9$)(η^5-7,8-Me$_2$-7,8-C$_2$B$_9$H$_8$-10-Et)] (**13b**) (0.13 g). Anal. Calcd for C$_{27}$H$_{66}$N$_2$B$_{18}$O$_2$W$_2$: C, 32.01; H, 6.57; N, 2.77. Found: C, 31.72; H, 6.73; N, 2.54.

Protonation of [NEt$_4$][W$_2$(μ-CC$_6$H$_4$Me-4)(CNBu^t)(CO)$_2$-(η^5-7,8-Me$_2$-7,8-C$_2$B$_9$H$_9$){η^5-7,8-Me$_2$-7,8-C$_2$B$_9$H$_8$-10-(CH$_2$C$_6$H$_4$Me-4)}] (13a). A rapidly stirred solution of **13a** (0.18 g, 0.15 mmol) in CH$_2$Cl$_2$ (15 mL) was treated with HBF$_4$·Et$_2$O (26 μL, 0.17 mmol) and the mixture allowed to stir for 10 min, after which it was preadsorbed onto silica gel (ca. 3 g) and transformed to the top of a silica gel chromatography column. Elution with CH$_2$Cl$_2$–petroleum ether (1:6) first removed a brown impurity followed by a blue fraction. Concentration in vacuo to ca. 5 mL and cooling (ca. −30 °C) gave blue *microcrystals* of [W$_2${μ-C(C$_6$H$_4$Me-4)CN(H)Bu^t}(CO)$_2$(η^5-7,8-Me$_2$-7,8-C$_2$B$_9$H$_9$){η^5-7,8-Me$_2$-7,8-C$_2$B$_9$H$_8$-10-(CH$_2$C$_6$H$_4$Me-4)}] (**14**) (0.09 g). Anal. Calcd for C$_{31}$H$_{55}$NB$_{18}$O$_2$W$_2$: C, 35.94; H, 5.35; N, 1.35. Found: C, 35.21; H, 4.84; N, 1.06.

Crystal Structure Determination. The crystal data and other experimental details for the compound [NEt$_4$][W$_2$(μ-CC$_6$H$_4$Me-4)(CO)$_2$(η^5-7,8-Me$_2$-7,8-C$_2$B$_9$H$_9$){η^6-7,8-Me$_2$-7,8-C$_2$B$_9$H$_8$-10-(CH$_2$C$_6$H$_4$Me-4)}] (**10a**) are given in Table V. Crystals were grown by the slow diffusion of petroleum ether into a CH$_2$Cl$_2$ solution of the complex at ca. 25 °C. The cell dimensions were determined from the setting angle values of 25 accurately centered reflections. Two check reflections measured every 2 h showed no significant variation over the period of data collection (<2.1%). After removal of these check intensity data, averaging of duplicate and equivalent measurements was performed, the systematic absences were deleted and corrections for Lorentz, polarization, and X-ray absorption effects were applied; the latter corrections was based on an empirical method employing nine high-angle ψ scan data.

The structure was solved by the heavy-atom Patterson method (W atoms), and successive difference Fourier syntheses were used to locate all the other non-hydrogen atoms which were refined with anisotropic thermal parameters. The hydrogen atom H(12b) was directly located in difference Fourier syntheses and allowed to ride on the atom B(12). All other hydrogen atoms were included at geometrically calculated positions (C–H 0.96, B–H 1.10 Å) using a riding model with fixed isotropic thermal parameters (U_{iso} 80 and 60 × 10^{-3} Å^2, respectively). Calculations were performed using the SHELXTL-PC package of programs.[22] Atomic scattering factors were taken from ref 23. Final atomic positional parameters for the non-hydrogen atoms are given in Table VI.

Acknowledgment. We thank the Robert A. Welch Foundation for support (Grants AA-1201 and 0668).

Supplementary Material Available: Complete tables of bond lengths and bond angles, anisotropic thermal parameters, and hydrogen atom parameters for **10a** (11 pages). Ordering information is given on any current masthead page.

OM920342G

---

[22] Siemens (1989). SHELXTL-PC Siemens X-ray Instruments, Madison, WI.

[23] *International Tables for X-ray Crystallography*; Kynoch Press: Birmingham, UK, 1974; Vol. 4.